OPEN

Group 2 innate lymphoid cells utilize the IRF4-IL-9 module to coordinate epithelial cell maintenance of lung homeostasis

A Mohapatra[1,2], SJ Van Dyken[1,2], C Schneider[1,2], JC Nussbaum[1,2], H-E Liang[1,2] and RM Locksley[1,2]

Group 2 innate lymphoid cells (ILC2s) have an important role in acute allergic lung inflammation. Given their distribution and function, lung ILC2s are hypothesized to coordinate epithelial responses to the external environment; however, how barrier surveillance is linked to ILC2 activation remains unclear. Here, we demonstrate that alveolar type II cells are the main source of interleukin (IL)-33 and thymic stromal lymphopoietin (TSLP) generated in response to chitin or migratory helminths. IL-33 and TSLP synergistically induce an interferon regulatory factor 4 (IRF4)-IL-9 program in ILC2s, and autocrine IL-9 promotes rapid IL-5 and IL-13 production required for optimal epithelial responses in the conducting airways. Thus, ILC2s link alveolar function to regulation of airway flow, revealing a key interaction between resident lymphoid and structural cells that might underlie similar organizational hierarchies in other organs.

INTRODUCTION

Chitin is a polymer of *N*-acetylglucosamine that is abundant in the environment as a structural constituent of fungi, helminths, and arthropods.[1] When administered to the lungs of mice as insoluble beads, chitin induces an innate inflammatory response characterized by the rapid accumulation of eosinophils and alternatively activated macrophages around beads impacted in the distal airway.[2] This cellular influx is dependent on activation of interleukin (IL)-5 and IL-13 from resident lung group 2 innate lymphoid cells (ILC2s).[3] Like other innate lymphoid cells, ILC2s are dispersed widely in the body tissues of mice and humans, especially at the mucosal barriers of the lung, skin, nasopharynx, and bowel.[4] Disparate insults, such as influenza infection, that induce widespread epithelial lung damage also activate ILC2s,[5,6] suggesting a sentinel function for these cells.

In an earlier study, we detected acute production of the IL-1 family member IL-33 and the IL-7-like cytokine thymic stromal lymphopoietin (TSLP) in lung tissues after chitin challenge; the IL-17 family member IL-25 was induced transiently in bronchoalveolar lavage (BAL) fluid but not in tissue.[3] Roles for these cytokines in ILC2-dependent inflammation after chitin were revealed genetically.[3] Given the relatively low numbers of lung ILC2s and their tight clustering within broncho-vascular bundles,[7,8] however, the cellular sources of these signals and how ILC2s integrate them remain unclear. Here, we combine immunohistochemistry and cell fractionation experiments to localize acute IL-33 and TSLP after chitin challenge to the alveolar type II (ATII) cells of the distal airway, establishing that these signals are spatially and temporally co-regulated. IL-33 and TSLP synergistically activate lung ILC2s, inducing a cell-intrinsic interferon regulatory factor 4 (IRF4)-IL-9 effector program. Autocrine IL-9 rapidly generates IL-5, IL-13 and subsequent conducting airway proteins that drive tissue defense and repair. These studies thereby link ILC2 activation to epithelial cells that monitor alveolar integrity and tissue responses that regulate airway flow. This model might underpin the role of ILCs in other tissues, where their small numbers and restricted localization may reflect similar organizational hierarchies.

RESULTS

ATII cells are the source of IL-33 and TSLP in response to chitin

We previously reported increased IL-33 and TSLP protein in whole lung homogenates from BALB/c mice 6–12 h after chitin

[1]Departments of Microbiology and Immunology and Medicine, University of California, San Francisco, California, USA and [2]Howard Hughes Medical Institute, University of California, San Francisco, California, USA. Correspondence: RM Locksley (locksley@medicine.ucsf.edu)

Received 16 February 2015; accepted 27 May 2015; published online 1 July 2015. doi:10.1038/mi.2015.59

challenge.[3] C57BL/6 mice developed similar increases in IL-33 and TSLP after 6 h; induction of IL-33 was sustained, whereas TSLP transiently increased (**Figure 1a**). Neither cytokine was elevated in mice given phosphate-buffered saline (PBS) or polystyrene beads (**Supplementary Figure S1a** online) or detected in BAL fluid (data not shown). Increased TSLP protein was associated with transcription, but chitin did not affect *Il33*, *Il7,* or *Il2* transcripts (**Figure 1b**). Further, IL-33 was expressed in the nuclei of lung cells positive for the ATII cell marker surfactant protein C (SPC) in unchallenged mice (**Figure 1c**); this localization remained unchanged after chitin administration (**Supplementary Figure S1b**). These data are consistent with chitin-induced, post-transcriptional modification of a constitutive IL-33 pool. To address this possibility, we assessed IL-33 in lung homogenates from naïve and chitin-challenged mice by western blot. A ~35-kDa band, corresponding to full-length IL-33, was present in all homogenates, together with a ~20-kDa band, corresponding to a C-terminal fragment; neither band was detected in homogenates from *Il33*$^{-/-}$ mice (**Figure 1d**). Although total IL-33 increased with chitin (**Figure 1a**), 20-kDa (and smaller) fragments comprised a larger proportion (**Figure 1e**), consistent with proteolytic processing after chitin challenge.

Conversely, we could not detect TSLP in the lung using immunohistochemical methods (data not shown). As an alternative approach, we sorted lung hematopoietic and epithelial populations from resting and chitin-challenged mice (**Supplementary Figure S1c** and **Figure 1f**). We could only detect TSLP protein by ELISA in CD45^{lo} EpCAM^{+} cells isolated from chitin-challenged mice (**Figure 1g**), although other sorted populations expressed *Tslp* transcripts (**Supplementary Figure S1d**). Post-sort and cytospin analyses revealed that these cells were highly granular and positive for SPC, as are ATII cells (**Figure 1f**).[9] Consistent with this finding, SPC^{+} MLE12 lung epithelial cells[10] also expressed TSLP after stimulation (**Figure 1g**). Thus, ATII cells comprise the major source of IL-33 in the resting mouse lung and of TSLP rapidly after chitin challenge.

TSLP and IL-33 cooperatively activate ILC2s *in vivo*

The overlapping temporal and spatial expression of IL-33 and TSLP in response to chitin suggested these cytokines might function cooperatively. We modeled this by intranasally administering cytokine and analyzing the lung infiltrate after 12 h. Although TSLP or IL-33 elicited little eosinophil influx when administered alone at modest doses, a combination of both cytokines resulted in significantly increased eosinophil accumulation (**Figure 2a and d**). The combination also elicited increased surface CD25 expression on ILC2s, consistent with their activation (**Figure 2b**); ILC2 frequencies, however, remained unchanged (**Figure 2d**). Next, we administered IL-33 and TSLP to the lungs of mice homozygous for the *Il5*^{red5} reporter allele, in which a sequence encoding tdTomato is present at the *Il5* start site.[8] We observed modest increases in IL-5 expression by ILC2s after IL-33 or TSLP alone but a significant increase with the combination (**Figure 2c**); IL-13 was similarly induced in BAL fluid in *Il4ra*$^{-/-}$ mice (**Supplementary Figure S2**). Thus, IL-33 and TSLP function cooperatively at modest doses *in vivo* to activate ILC2s, increase their cytokine production and drive eosinophil accumulation.

TSLP synergizes with IL-33 to stimulate ILC2s

To investigate the interaction of IL-33 and TSLP in a cell-intrinsic manner, we purified lung ILC2s from resting mice and measured cytokine release into the supernatant after 3 days of culture (**Supplementary Figure S3**). Although IL-33 (10 ng ml^{-1}) induced barely detectable amounts of IL-5, IL-13, and IL-9, the addition of 0.1 ng ml^{-1} TSLP significantly increased production; no cytokines were detected when ILC2s were cultured with TSLP alone, even at 100-fold higher concentrations (**Figure 3a**). TSLP, IL-2, and IL-7 each synergized comparably with IL-33 to induce ILC2 cytokines (**Figure 3b**). Responses to IL-33 and TSLP were detected at 16 h by mRNA and protein, but were absent in ILC2s lacking receptors for IL-33 (IL1RL1) and TSLP (TSLPR; data not shown). Thus, IL-33 and TSLP synergistically induce a cell-intrinsic program of effector cytokine production in lung ILC2s.

ILC2-derived IL-9 requires IRF4 and amplifies cell-intrinsic cytokine production *in vitro*

ILC2s constitutively express high levels of the IL-9 receptor, IL9R,[11,12] suggesting that autocrine signaling might explain the marked synergy of IL-33 and TSLP in ILC2 activation. To investigate this, we generated IL-9-enhanced yellow fluorescent protein (YFP) reporter (9er) mice, in which the endogenous *Il9* translation initiation site is replaced with YFP sequence linked by an internal ribosome entry site to a sequence

Figure 1 Alveolar type II (ATII) cells are the source of interleukin (IL)-33 and thymic stromal lymphopoietin (TSLP) in response to chitin. (**a**) ELISA of IL-33 (left) and TSLP (right) from whole lung homogenates of mice at indicated times after chitin administration. (**b**) Quantitative reverse transcription-PCR analysis of *Il33, Tslp, Il2,* and *Il7* expression from whole lung RNA of mice 6 h after chitin challenge. Values normalized to *18s* expression and graphed as fold increase over the mean of the 0 h mice. (**c**) Immunohistochemistry of naive mouse lungs. Original magnification, ×200. Scale bar, 50 μm. (**d**) Western blot analysis of whole lung homogenates of mice at indicated times after chitin. "rIL-33" is recombinant protein (Ser109-Ile266; R&D Systems). IB, immunoblot. (**e**) Ratio of 20-kDa anti-IL-33-reactive band pixel density to total IL-33 pixel density (sum of 20-kDa band and 35-kDa band densities) in each lane, compiled from three independent experiments. (**f**) Flow cytometry (left) and immunocytochemistry (right) of post-sort ATII cells (DAPI^{lo} CD45^{lo} CD11b^{lo} CD31^{lo} EpCAM^{+}) isolated from lungs of mice 3 h after chitin. Original magnification, ×200. Scale bar, 10 μm. (**g**) ELISA of TSLP in lung populations sorted from mice 3 h after PBS or chitin (left) and in supernatants from MLE12 cells cultured with 40 ng ml^{-1} phorbol 12-myristate 13-acetate for the indicated times (right), compiled from four independent experiments, respectively. Where applicable: $^{*}P<0.05$, $^{**}P<0.005$, $^{***}P<0.0005$ and NS, not significant (two-tailed *t*-test). Data are representative of at least three independent experiments with 2–4 mice per exposure (**a**,**f**) or at least two independent experiments with 3 mice per exposure (**b**–**d**). DAPI, 4',6-diamidine-2'-phenylindole dihydrochloride; SPC, surfactant protein C.

encoding optimized Cre recombinase (**Figure 4a**). When activated under conditions that promote IL-9 expression, naïve CD4$^+$ T cells from *Il9*$^{9er/9er}$ mice express YFP instead of IL-9, confirming that *Il9*$^{9er/9er}$ mice are IL-9-deficient (**Figure 4b** and **Supplementary Figure S4a**). Further, Cre-driven lineage tracing in *Il9*$^{9er/9er}$; *ROSA26*$^{fl\text{-}STOP\text{-}eYFP/+}$ mice demonstrated that ILC2s were the major lung source of IL-9 in unchallenged, adult mice (**Supplementary Figure S4b**). To test whether IL-9 deficiency has cell-intrinsic effects, we purified lung ILC2s from wild-type and *Il9*$^{9er/9er}$ mice and cultured

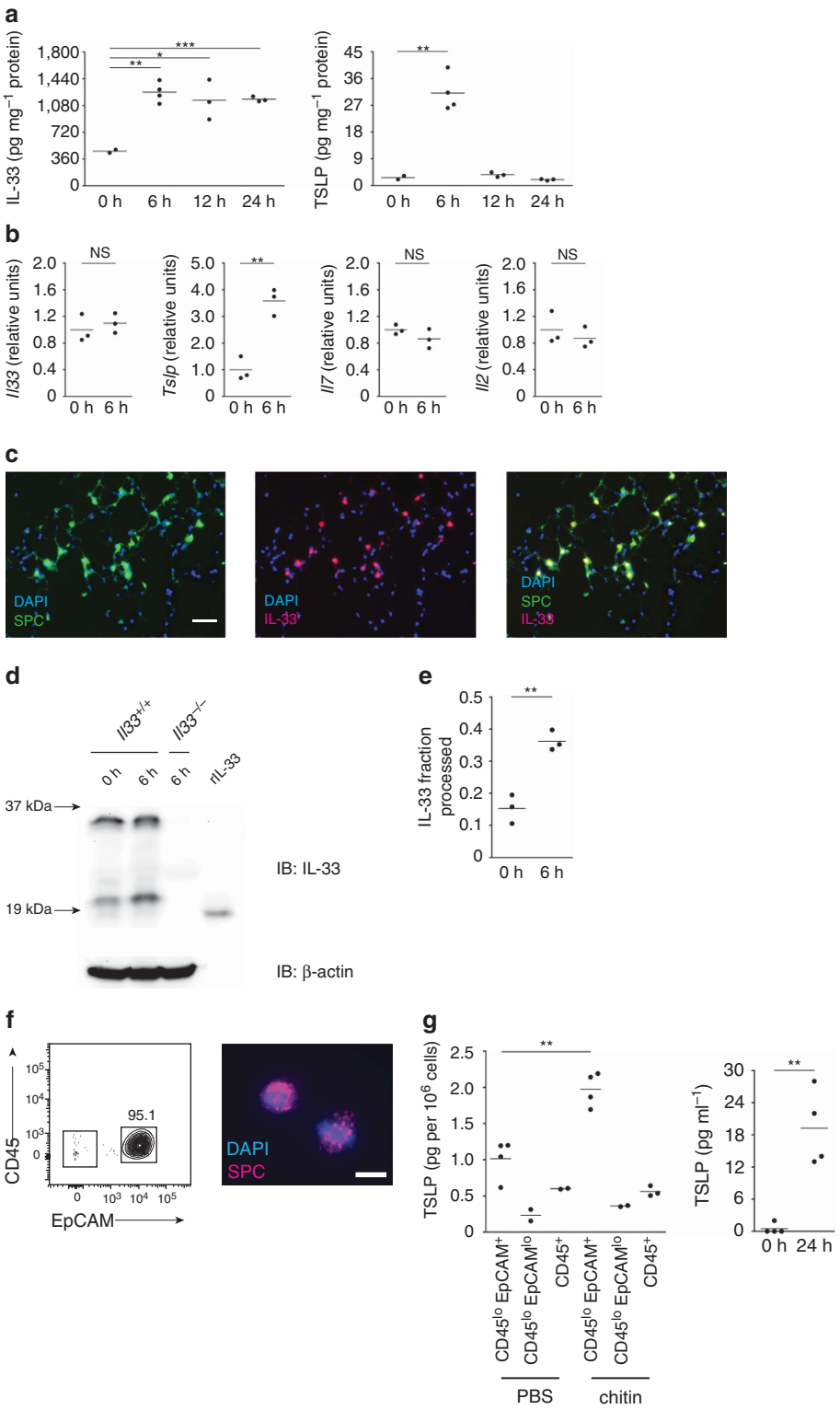

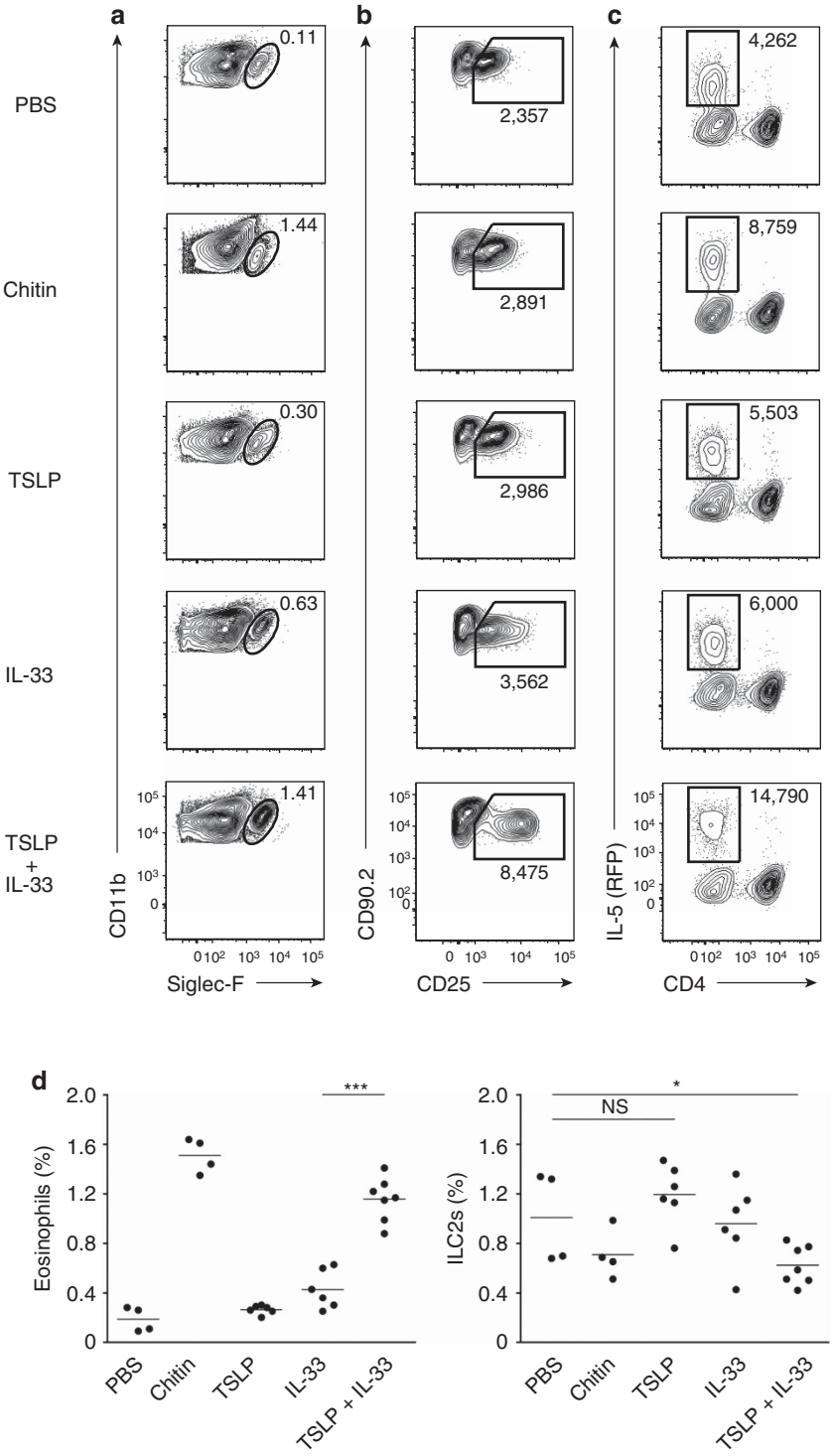

Figure 2 Thymic stromal lymphopoietin (TSLP) and interleukin (IL)-33 cooperatively activate group 2 innate lymphoid cells (ILC2s) *in vivo*. Mice were analyzed 12 h after administration of phosphate-buffered saline (PBS), chitin, 1 μg rTSLP (recombinant TSLP), 50 ng rIL-33, or rTSLP + rIL-33. (**a**–**c**) Flow cytometry of eosinophils (**a**; pre-gate: DAPI^{lo} CD11c^{lo}) and ILC2s (**b**, **c**; pre-gate: DAPI^{lo} CD11c^{lo} CD11b^{lo} thy1.2^{+} CD8^{lo} B220^{lo} NK1.1^{lo} CD4^{lo}) from the lungs of wild-type mice (**a**,**b**) or *Il5*$^{red5/red5}$ mice (**c**). Numbers near gates represent percentage of live cells (DAPI^{lo} CD11c^{lo} CD11b^{+} SSC^{hi} Siglec-F^{+} α4β7^{lo}; **a**) or mean fluorescence intensity (**b**,**c**). (**d**) Eosinophils (left) and ILC2s (right) graphed as a percentage of live cells, gated as in **a** and **b**, respectively. Where applicable: *$P<0.05$, ***$P<0.0005$, and NS, not significant (two-tailed *t*-test). Representative flow cytometry data from two independent experiments with 2–4 mice per exposure is shown in **a**–**c**, with compiled results in **d**.

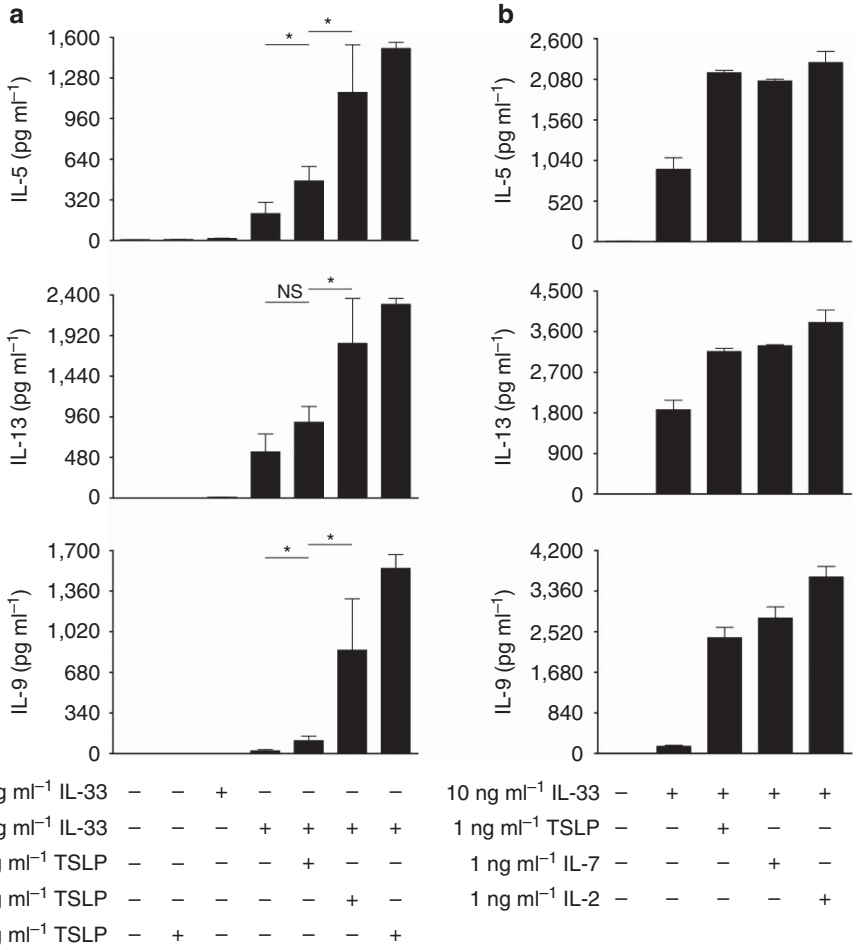

Figure 3 Thymic stromal lymphopoietin (TSLP) synergizes with interleukin (IL)-33 to stimulate group 2 innate lymphoid cells (ILC2s). Lung ILC2s were sorted from wild-type mice and cultured for 3 days. Expression of IL-5, IL-13, and IL-9 in supernatants after stimulation with IL-33 and/or TSLP (**a**) or with IL-33 and either TSLP, IL-7, or IL-2 (**b**) was assessed by cytometric bead array. Where applicable: $*P<0.05$ and NS, not significant (two-tailed *t*-test). Data are representative of at least three independent sorts of cells pooled from multiple mice. Bars represent mean + standard deviation. The mean is the average of duplicate or triplicate wells per condition.

them with IL-33 and TSLP for 3 days. *Il9*$^{9er/9er}$ ILC2s produced no IL-9 (**Figure 4c**) and substantially less IL-5 and IL-13 than did wild-type cells, and this deficit was restored by addition of exogenous IL-9 (**Figure 4e**). Genotype did not affect number of cells recovered under any culture conditions tested (**Figure 4e**), and IL-9-deficient ILC2s did not express reduced amounts of IL1RL1 or TSLPR at baseline (**Supplementary Figure S6a**).

Production of IL-9 in helper T cells requires IRF4,[13] but the role of this transcription factor in ILC2s is unclear. We bred *Irf4*$^{fl/fl}$ mice, in which exons 1 and 2 are flanked by *loxP* sites,[14] to CMV-Cre transgenic mice to generate *Irf4*$^{-/-}$ mice (**Supplementary Figure S5**) and confirmed that lung ILC2s constitutively express IRF4 by flow cytometry (**Figure 4d**). *Irf4*$^{-/-}$ ILC2s cultured with IL-33 and TSLP for 3 days were viable and expressed IL-9, IL-5, and IL-13 in a manner identical to that of *Il9*$^{9er/9er}$ cells; diminished IL-5 and IL-13 expression in *Irf4*$^{-/-}$ ILC2s could be rescued by addition of IL-9 (**Figure 4e**). Furthermore, in mixed, 3-day cultures of *Il5*$^{red5/red5}$ ILC2s (which express tdTomato instead of IL-5[8]) and *Il9*$^{9er/9er}$ ILC2s with IL-33 and TSLP, we observed restored IL-5 production, suggesting that IL-9 from nearby ILC2s can induce cytokine production in neighboring cells (**Figure 4f**). Thus, ILC2-derived IL-9 requires IRF4 and acts in an autocrine manner to optimize IL-5 and IL-13 production.

IRF4 and IL-9 are required for rapid, ILC2-mediated lung epithelial responses *in vivo*

Our results demonstrating that ATII cells rapidly produce TSLP and IL-33 after chitin, together with our observation that these cytokines synergize to induce IL-9 in ILC2s, raised the possibility that chitin induces early IL-9 important for rapid and robust effector function. Indeed, we observed expression of *Il9* transcripts in the lungs of mice 1 day after chitin that was not explained by any change in the number of lung ILC2s (**Figure 5a and b**). Moreover, IL-9-deficient mice had reduced induction of *Il13* transcripts as compared with

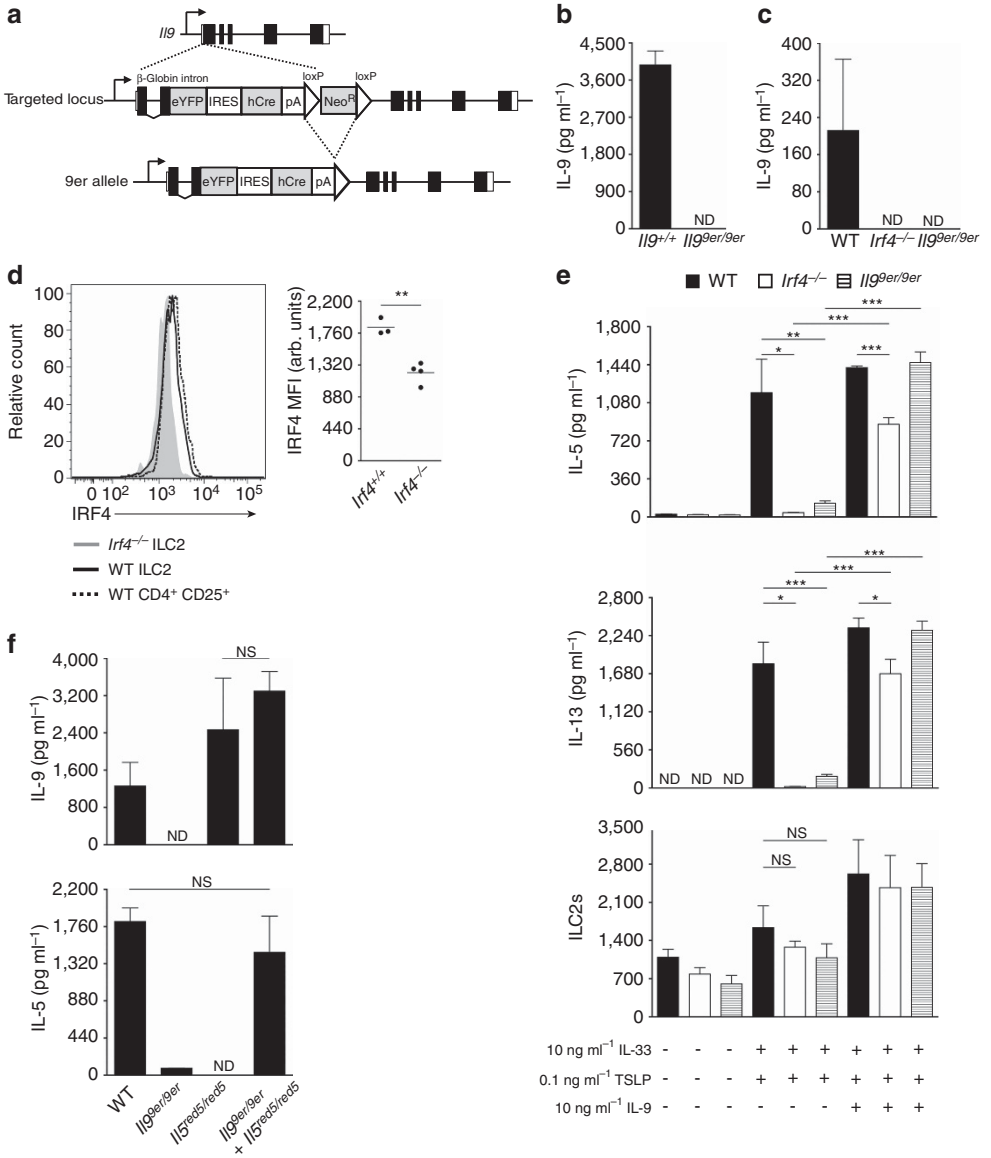

Figure 4 Group 2 innate lymphoid cell (ILC2)-derived interleukin (IL)-9 requires interferon regulatory factor 4 (IRF4) and amplifies cell-intrinsic cytokine production *in vitro*. (**a**) Gene targeting schematic for generation of the $Il9^{9er}$ allele. (**b**) Expression of IL-9 by cytometric bead array (CBA) in supernatants from 4-day "Th9" cultures of naïve CD4$^+$ T cells sorted from $Il9^{+/+}$ and $Il9^{9er/9er}$ mice. (**c**) Expression of IL-9 by CBA in supernatants from 3-day cultures of lung ILC2s with 0.1 ng ml^{-1} rTSLP and 10 ng ml^{-1} rIL-33, sorted from wild-type (WT), $Irf4^{-/-}$, and $Il9^{9er/9er}$ mice. (**d**) IRF4 expression (left) in ILC2s and CD4$^+$ CD25$^+$ T cells from the lungs of naive $Irf4^{+/+}$ and $Irf4^{-/-}$ mice, as assessed by flow cytometry; median fluorescence intensities (MFIs) of IRF4 staining in ILC2s are graphed at right. (**e**) Expression of IL-5 and IL-13 by CBA in supernatants from 3-day cultures of lung ILC2s with the indicated cytokines, sorted from WT, $Irf4^{-/-}$, and $Il9^{9er/9er}$ mice. Number of LiveDead^{lo} cells by FACS recovered at the end of culture is graphed below. (**f**) Expression of IL-5 and IL-9 by CBA in supernatants from 3-day cultures of lung ILC2s with 0.1 ng ml^{-1} rTSLP and 10 ng ml^{-1} rIL-33. Wells contained 5,000 cells of the indicated genotype or 10,000 cells (last column, 5,000 per genotype). Where applicable: $^*P<0.05$, $^{**}P<0.005$, $^{***}P<0.0005$, and NS, not significant (two-tailed *t*-test). ND, not detected. Bars represent mean + standard deviation. The mean is the average of duplicate or triplicate wells per condition, with individual wells seeded with cells from a single mouse (**c**, **e**) or a pool of mice (**b**, **f**). Data in **b**, **c**, **e** and **f** are representative of at least two independent sorts with 2–4 mice per genotype; in **d**, of at least two independent experiments with at least 3 mice per genotype.

wild-type mice, although induction of *Il5* was not affected under these conditions (**Figure 5b**).

We turned to a second model of allergic lung inflammation to explore the generalized nature of these findings. Hours after subcutaneous inoculation, the helminth *Nippostrongylus brasiliensis* reaches the mouse lung and molts before rupturing into the alveolar sacs and ascending the trachea to complete its migration to the small intestine. Epithelial injury induced during this period is associated with chitin turnover during synthesis of the pharynx.[15,16] *N. brasiliensis* infection elicited TSLP and IL-33 protein in BAL fluid 1 day after infection; both cytokines returned to near baseline by 4 days (**Figure 5c**) and expression was not affected by IL-9 or IRF4 deficiency (**Supplementary Figure S6b**). Western blot for IL-33 in

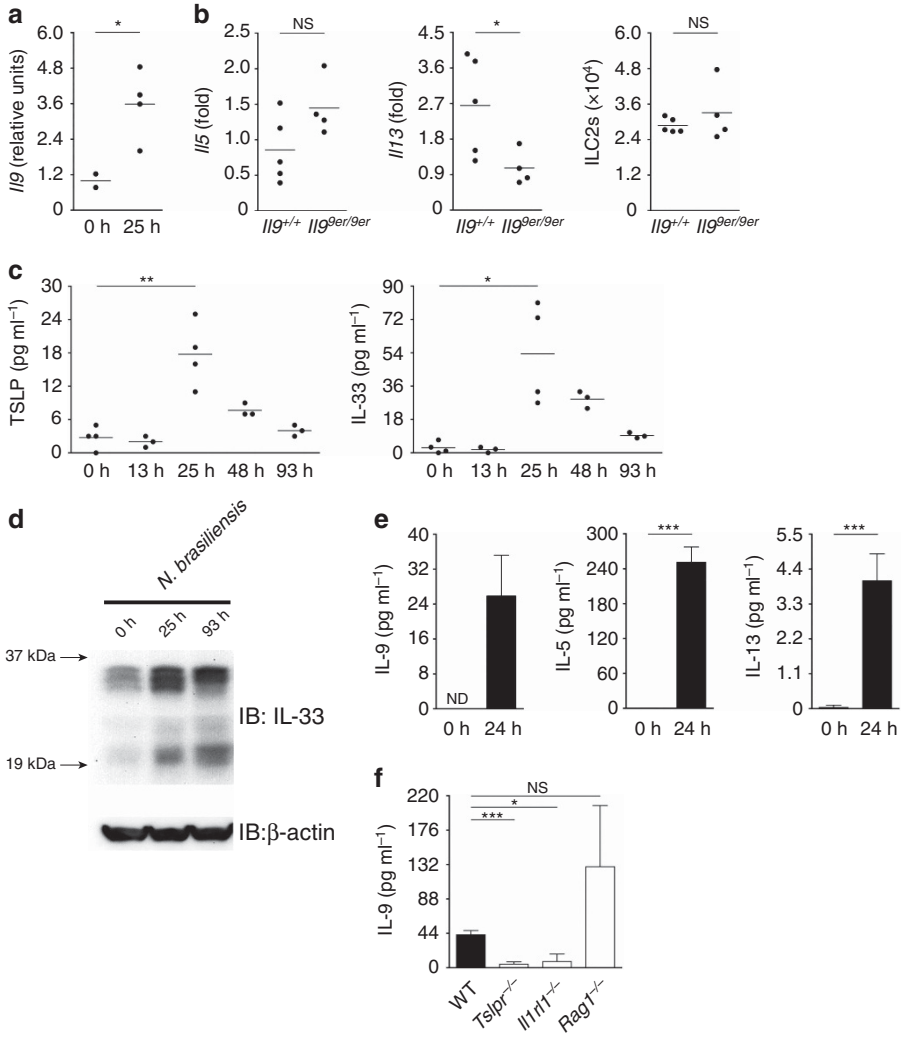

Figure 5 Early interleukin (IL)-9 augments rapid group 2 innate lymphoid cell (ILC2) cytokine expression in response to chitin or *N. brasiliensis* challenge. (**a**) Quantitative reverse transcription-PCR (RT-PCR) analysis of whole lung RNA from mice at the indicated times after chitin, normalized to *18 s* expression, and graphed in arbitrary units. (**b**) Quantitative RT-PCR analysis of *Il5* (left) and *Il13* (middle) expression and enumeration of ILC2s by flow cytometry (right) in the lungs of $Il9^{+/+}$ or $Il9^{9er/9er}$ mice 25 h after chitin. RT-PCR values are normalized to *18 s* expression and presented as fold increase over normalized values in unexposed mice (not shown). (**c**) ELISA of thymic stromal lymphopoietin (TSLP) and IL-33 from bronchoalveolar lavages (BALs) of mice at the indicated times after *N. brasiliensis* infection. (**d**) Western blot analysis of whole lung homogenates from mice at the indicated times after challenge with *N. brasiliensis* or chitin. IB, immunoblot. (**e**) Cytometric bead array (CBA) analysis of IL-9, IL-5, and IL-13 in BALs from mice at the indicated times after *N. brasiliensis* infection. (**f**) CBA analysis of BALs from mice of the indicated genotypes 24 h after *N. brasiliensis* infection. Where applicable: $^{*}P<0.05$, $^{**}P<0.005$, $^{***}P<0.0005$ and NS, not significant (two-tailed *t*-test). Data in **a** are compiled from two independent experiments; in **b**–**d**, representative of two experiments with 2–5 mice per exposure. Data in **e** and **f** are compiled from three independent experiments, with each data point representing BALs pooled from 3–5 mice; bars represent mean + standard deviation. ND, not detected.

lung homogenates from infected mice revealed accumulation of ~35-kDa and ~20-kDa bands identical to those observed following chitin challenge (**Figure 5d**). Concordant with detection of TSLP and IL-33, we detected IL-9, IL-5, and IL-13 in BAL fluid 1 day after infection (**Figure 5e**), and ILC2s sorted from the lungs of these mice expressed these cytokines when cultured overnight without further stimulation (**Supplementary Figure S6c**). Recombination Activating Gene 1-deficient mice had readily detectable IL-9 production in BAL fluid 24 h after infection, whereas significantly less IL-9 was recovered from the lungs of mice deficient in either TSLPR or IL1RL1 (**Figure 5f**). These data are consistent with ILC2-derived cytokine production independent of and before T cell infiltration of the lungs at day 4–5 after *N. brasiliensis* infection.[17]

To determine whether early IL-5 and IL-13 expression was dependent on IRF4 and IL-9, we assessed the lungs of wild-type, $Irf4^{-/-}$, and $Il9^{9er/9er}$ mice on day 3 after infection. $Irf4^{-/-}$ and $Il9^{9er/9er}$ mice had significantly fewer lung eosinophils than did wild-type mice on day 3, despite having equivalent numbers of lung ILC2s (**Figure 6a**). ILC2s sorted from infected mice and deficient in IRF4 or IL-9 also produced significantly less IL-5 or IL-13 in overnight *ex vivo* cultures (**Figure 6b**). Moreover, transcripts of *Il5* and *Il13* and of IL-13 target genes known to be expressed in lung epithelial cells to promote mucus production and tissue repair, including *Muc5ac*, *Clca3,* and *Tff2*,[18,19] were

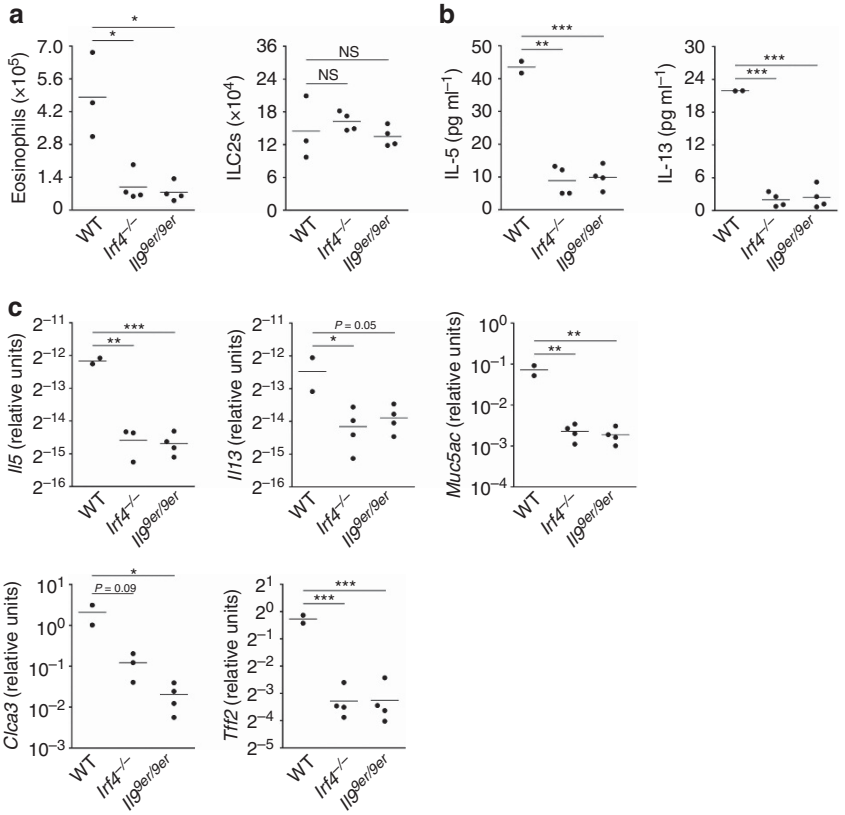

Figure 6 Interferon regulatory factor 4 (IRF4) and interleukin (IL)-9 are required for the rapid, group 2 innate lymphoid cell (ILC2)-mediated lung epithelial response to *N. brasiliensis*. Wild-type (WT), *Irf4*$^{-/-}$, and *Il9*$^{9er/9er}$ mice were infected with *N. brasiliensis*, and lungs were harvested 3 days later. (**a**) Flow cytometric analysis of eosinophils (DAPI^{lo} CD11c^{lo} CD11b^{+} SSC^{hi} Siglec-F^{+}; left) and ILC2s (DAPI^{lo} CD11c^{lo} CD11b^{lo} CD8^{lo} B220^{lo} thy1.2^{+} CD5^{lo} CD4^{lo} CD45^{+} CD25^{+}; right). (**b**) Cytometric bead array analysis of supernatants from 16 h, *ex vivo* cultures of lung ILC2s sorted from infected mice of the indicated genotypes. (**c**) Quantitative reverse transcription-PCR analysis of whole lung RNA for expression of *Il5*, *Il13,* and IL-13 target genes, normalized to *18s* expression and graphed in arbitrary units. Where applicable: *$P<0.05$, **$P<0.005$, ***$P<0.0005$, and NS, not significant (two-tailed *t*-test). Data are representative of at least two experiments with 2–4 mice per genotype.

significantly reduced in mice lacking IRF4 or IL-9 (**Figure 6c**). Thus, IL-9 from lung ILC2s is generated in a rapid, IRF4-dependent manner *in vivo* and is required for optimal ILC2 elaboration of IL-5 and IL-13, which drives subsequent eosinophilia and supports epithelial defense and repair.

DISCUSSION

We used two models of localized lung injury—chitin bead impaction and migratory helminth infection—to define a novel cell and cytokine pathway that links alveolar damage, activation of ILC2s, and airway homeostasis. We identify IL-33 and TSLP as requisite early cytokines generated by epithelial ATII cells with contemporaneous expression patterns. Co-expression of IL-33 and TSLP synergistically induced an IRF4-IL-9 program in ILC2s, in which IL-9 sustained autocrine amplification of IL-5 and IL-13 production. In the absence of IRF4 or IL-9, IL-13-dependent expression of epithelial genes involved in barrier responses, including increases in mucus and enzymatic chitinase and promotion of repair,[18–21] was abrogated. Thus, ILC2s integrate signals from specialized epithelial cells that monitor alveolar function to rapidly mediate barrier alterations in conducting airway epithelia.

The presence of constitutive, nuclear IL-33 in the lung epithelial cells of resting mice has been noted, as has transcriptional induction in a variety of resident and recruited cells during inflammation.[19,22] The mechanism by which the active, C-terminal, IL-1-like domain of IL-33 is released from chromatin to signal neighboring cells remains unclear, however.[23–25] Here, we demonstrate that a ~20-kDa protein, reactive with antibodies raised against Ser109-Ile266 of mouse IL-33 (R&D Systems), accumulates *in vivo* after chitin or helminth exposure. The increase in total IL-33, evident by ELISA and western blotting, may reflect a subtle increase in full-length protein expression combined with rapid processing or increased recovery from inflamed lung samples. Processed IL-33 also accumulates in oleic acid-induced lung damage[23] and in RIPK1-deficient mice that die of uncontrolled necroptosis,[26] consistent with injury as an elicitor of processing. Intriguingly, we also identified ATII cells as the predominant source of TSLP after challenge with chitin or migratory worms. TSLP has been detected by transcript profiling in various cells at mucosal

sites,[27] consistent with our findings. Our observation of discordance between mRNA and protein expression suggests, however, that post-transcriptional regulation of TSLP may be an important mechanism of control.[28]

Synergistic activation of lung ILC2s by combinations of IL-33 with TSLP, IL-2, or IL-7 has been described *in vitro*.[12,29,30] Here, we used two distinct *in vivo* challenges to demonstrate acute induction of IL-33 and TSLP, but not IL-2 or IL-7, and observed direct synergy between them. This synergy may explain how these cytokines can potently activate ILC2s across large diffusion gradients from the distal airway to lung broncho-vascular bundles.[7,8] IL-2 and IL-7 may be more relevant during the adaptive phases of inflammation.[12] Recent studies implicating both IL-33[31] and TSLP[32] in human asthma are consistent with our data. ILC2-derived IL-9, robustly induced by the combination of IL-33 and TSLP via IRF4, was the mediator of synergistic ILC2 activation, revealing a mechanism for rapid cytokine expression through autocrine signaling. Our novel observation that IRF4 is required for ILC2 effector function is consistent with the role of this transcription factor in a larger chromatin-modifying complex that regulates cytokine production in Th9, Th2, and Th17 cells.[13,33] Whereas previous studies linked IL-9 to late lung repair[34] and adaptive Th9-mediated worm immunity,[17] our data demonstrate a novel role for IL-9 in acute stabilization of mucosal homeostasis, as IL-13-mediated epithelial responses were highly attenuated in its absence. These data also explain previous observations linking transgenic IL-9 expression to epithelial gene transcription via IL-13 from hematopoietic cells.[35]

Although they constitute 60% of the alveolar epithelium, ATII cells are estimated to cover only 5% of the alveolar surface,[9] suggesting that they complement the gas exchange role of type I cells in unique ways. Indeed, ATII cells have been implicated in surfactant homeostasis, microbial defense,[9] clearance of apoptotic cells,[36] and alveolar regeneration.[37] Our finding that ATII cells are the major source of IL-33 and TSLP involved in the acute lung challenges investigated here supports a role for these cells as alveolar sentinels and focuses interest on the upstream signals that induce release of these cytokines. Multiple pathways, including physicochemical,[38,39] metabolic,[40,41] and structural[42] elements, are the focus of further study, with different inputs potentially underlying each cytokine. The physical circuits by which these signals are transmitted also remain unclear. Our data position lung ILC2s in a pathway between specialized epithelial cells that sense and regulate alveolar functions, such as gas exchange, and conducting airway cells that control access to alveoli. Interactions between resident innate lymphoid cells and structural cells, likely established during tissue development,[8] may define a generalized framework for homeostasis in other organs.

METHODS

Mice. Wild-type C57BL/6J, *ROSA26*$^{fl\text{-}STOP\text{-}eYFP}$, *Irf4*$^{fl/fl}$, and *Rag1*$^{-/-}$ mice were obtained from. The Jackson Laboratory (Bar Harbor, ME). *Il33*$^{Gt/Gt}$ (IL-33-deficient),[43] *Tslpr*$^{-/-}$,[44] and *Il1rl1*$^{-/-}$[45] mice were generous gifts from J-P Girard (University de Toulouse), S Ziegler (Benaroya Research Inst.), and M Steinhoff (University of California, San Francisco), respectively. Other strains used include *Il5*$^{red5/red5}$ (ref. 8) and *Il4*$^{4get/4get}$.[46] Mice were backcrossed to C57BL/6J for at least 10 generations and maintained in the UCSF-specific pathogen-free animal facility in accordance with guidelines established by the Institutional Animal Care and Use Committee and Laboratory Animal Resource Center. All experiments were performed on 6- to 12-week-old mice.

IL-9 reporter (9er) mice were generated by homologous gene targeting in C57BL/6 embryonic stem cells (PRXB6T). We used a reporter cassette derived from the pKO915-DT plasmid (Agilent, Santa Clara, CA), containing (in order from 5′ to 3′) genomic sequence for rabbit β-globin gene partial exons 2–3, enhanced YFP (Clontech, Mountain View, CA), encephalomyocarditis virus internal ribosome entry site (IRES), humanized Cre recombinase, bovine growth hormone poly(A), and *loxP*-flanked neomycin resistance. Homologous arms straddling the *Il9* translation initiation site (3.4 kb 5′, containing the promoter and 5′ untranslated region, and 3.0 kb 3′, containing the start ATG through 3′ untranslated region) were amplified from C57BL/6 genomic DNA using Phusion polymerase (Thermo Fisher Scientific, Waltham, MA) and ligated into the modified pKO915-DT plasmid, flanking the reporter cassette. The construct was linearized with *Not*I and transfected by electroporation into C57BL/6 embryonic stem cells. Cells were grown on irradiated feeders with media containing G418, and neomycin-resistant clones were screened for 5′ and 3′ homologous recombination by PCR. Two of 10 positive clones were injected into albino C57BL/6 blastocysts to generate chimeras, and male pups from a single clone were bred with homozygous CMV-Cre transgenic C57BL/6 females (The Jackson Laboratory) to excise the neomycin-resistant cassette. Males from this cross were bred to wild-type C57BL/6 females to remove the CMV-Cre allele.

***In vivo* challenges**. Purified chitin (New England Biolabs, Ipswich, MA) and 60-μm polystyrene beads (Polysciences, Warrington, PA) were prepared and administered as described.[3] Carrier-free, recombinant TSLP and IL-33 (R&D Systems, Minneapolis, MN) were reconstituted in sterile PBS and administered intranasally in 50 μl doses. Third-stage larvae of *N. brasiliensis* were prepared and administered under isoflurane anesthesia as described.[47]

Lung preparation. For BAL collection, lungs were instilled intratracheally with 1 ml PBS. The lavage fluid was centrifuged, and the supernatant was concentrated using Amicon Ultra filters (MWCO 10 kDa; EMD Millipore, Billerica, MA).

For flow cytometry or sorting of ILC2s, lungs were perfused with 10 ml PBS via the right ventricle. Lung lobes were excised and processed with a gentleMACS automated tissue dissociator in C tubes (Miltenyi Biotec, San Diego, CA), running program "m_lung_01", followed by shaking incubation for 30 min at 37 °C, 200 r.p.m., in Hanks' balanced salt solution (HBSS) (with Ca^{2+}, Mg^{2+}) containing 0.26 Wunsch units per ml Liberase TM and 25 μg ml^{-1} DNase I (Roche, Basel, Switzerland). Following incubation, a second dissociation was performed with program "m_lung_02".

For flow cytometry or sorting of ATII cells, lungs were instilled with 2 ml protease solution (300 U ml^{-1} collagenase Type I (Thermo Fisher Scientific), 4 U ml^{-1} elastase (Worthington Biochemical Corp., Lakewood, NJ), 5 U ml^{-1} dispase (Thermo Fisher Scientific), and 200 U ml^{-1} DNase I in HBSS), minced by razor, and incubated in a total volume of ~2.5 ml (with protease solution) in a shaker for 25 min at 37 °C, 200 r.p.m. Suspension was washed in PBS with 3% fetal bovine serum (Atlanta Biologicals, Flowery Branch, GA), washed in HBSS, and resuspended in 2 ml HBSS with 0.1% Trypsin-EDTA (Thermo Fisher Scientific) + 200 U ml^{-1} DNase I for 20 min at 37 °C, 200 r.p.m. The protocol was adapted from Rock *et al.*[48]

Following tissue dissociation, cell suspensions were filtered through a 70-μm nylon mesh, washed, and treated with ACK solution to lyse

red blood cells before final suspension in PBS with 3% fetal bovine serum. Cells were stained for flow cytometry or sorting.

Flow cytometry and sorting. Monoclonal, murine-specific antibodies from BioLegend (San Diego, CA) included: anti-CD11c (N418), anti-CD11b (M1/70), anti-Gr-1 (RB6-8C5), anti-CD19 (6D5), anti-CD4 (RM4-5), anti-CD8α (53-6.7), anti-CD25 (PC61), anti-NK1.1 (PK136), anti-Thy1.2 (53-2.1), anti-CD45.2 (104), anti-EpCAM (G8.8), and anti-CD45 (30-F11). Antibodies from eBioscience (San Diego, CA) included: anti-CD11b (M1/70), anti-CD4 (RM4-5), anti-CD8α (53-6.7), anti-Thy1.2 (53-2.1), anti-F4/80 (BM8), anti-CD49b (DX5), anti-CD5 (53-7.3), anti-CD45 (30-F11), anti-IRF4 (3E4), anti-GATA3 (TWAJ), anti-B220 (RA3-6B2), and anti-CD31 (390). Antibodies from BD Biosciences (San Jose, CA) included: anti-CD11c (HL3), anti-CD25 (PC61), anti-Thy1.2 (53-2.1), anti-Ly6G (1A8), anti-α4β7 (DATK32), and anti-Siglec-F (E50-2,440). An Alexa Fluor 488-conjugated anti-Siglec-F antibody was generated using purified anti-Siglec-F with an Alexa Fluor 488 monoclonal antibody labeling kit (Life Technologies).

Exclusion of 4',6-diamidine-2'-phenylindole dihydrochloride (Roche) or LiveDead (Thermo Fisher Scientific) identified live cells, which were enumerated with flow cytometric CountBright Absolute beads (Thermo Fisher Scientific), according to the manufacturer's instructions. Sample data were acquired with a LSRII flow cytometer (BD Biosciences) and analyzed using FlowJo software (Ashland, OR). Cells were sorted using a MoFlo XDP (Beckman Coulter, Brea, CA) instrument.

Cell culture. Sorted ILC2s were cultured (37 °C, 5% CO_2) at 5,000 cells per well in 100 µl (mixed cultures contained 5,000 cells per genotype) RPMI 1640 (Caisson Labs, North Logan, UT) containing 10% heat-inactivated fetal bovine serum, penicillin–streptomycin–L-glutamine, 2-mercaptoethanol (Bio-Rad Laboratories, Hercules, CA), and recombinant mouse cytokines (R&D Systems), as indicated. At harvest, cell-free culture supernatants were collected and cells were analyzed by flow cytometry. To assess intracellular protein expression, cells were fixed and permeabilized using the eBioscience Transcription Factor Staining Buffer Set.

MLE12 cells (American Type Culture Collection, Manassas, VA) were cultured (37 °C, 5% CO_2) in 1:1 DMEM:Ham's F-12 (Thermo Fisher Scientific) containing 10% heat-inactivated fetal bovine serum, penicillin–streptomycin–L-glutamine, and 2-mercaptoethanol. Cells were passaged with 0.05% Trypsin-EDTA and adhered for 24 h at 70% confluency, before exposure to phorbol 12-myristate 13-acetate (Sigma-Aldrich, St. Louis, MO) for 24 h. Culture supernatants were concentrated using Amicon Ultra filters.

Sorted naïve $CD4^+$ T cells were cultured (37 °C, 5% CO_2) at 2×10^6 cells per well in 2 ml RPMI 1640, prepared as described for ILC2 cultures. Wells were pre-coated with 5 µg ml^{-1} anti-CD3 and anti-CD28 antibodies 1 day before culture. For Th9 polarization, 20 ng ml^{-1} of recombinant mouse IL-2, 10 ng ml^{-1} of IL-4, and 10 ng ml^{-1} of transforming growth factor-β were added to wells for 4 days (R&D Systems). At harvest, culture supernatants were collected and cells were analyzed by flow cytometry as described above.

Immunohistochemistry. Lungs were inflated with 1:1 Tissue-Tek OCT (Sakura Finetek, Torrance, CA):PBS, and lobes were embedded in OCT, before frozen sectioning at 7 µm onto glass slides using a CM 3050S cryomicrotome (Leica Microsystems, Buffalo Grove, IL). Alternatively, sorted cells were spun onto glass slides using a Cytospin 2 cytocentrifuge (Thermo Fisher Scientific). After tissue adherence, slides were dehydrated in cold acetone. Goat anti-GFP (Abcam, Cambridge, UK), goat anti-mouse IL-33 (R&D Systems), and rabbit anti-mouse SPC (Abcam) antibodies were applied to sections and detected with fluorophore-conjugated anti-goat IgG and anti-rabbit IgG secondary antibodies (Thermo Fisher Scientific). Nuclei were counterstained with 4′, 6-diamidine-2′-phenylindole dihydrochloride (Roche). Images were acquired with an AxioCam HRm camera and an AxioImager M2 upright microscope (Carl Zeiss, Oberkochen, Germany).

Protein extraction and analysis. Lung lobes were snap-frozen in liquid nitrogen and later homogenized in TNT buffer with cOmplete Protease Inhibitor Cocktail (Roche) and Antifoam Y-30 (Sigma-Aldrich) in M tubes using gentleMACS, running program "Protein_01". The suspension was centrifuged for 5 min at 1,500 r.p.m., and the supernatant was incubated on ice for at least 30 min. Protein homogenate from sorted or cultured cells was prepared by triturating cell pellets in TNT buffer with protease inhibitor. Following incubation on ice for 30 min, suspensions were centrifuged at $16{,}100 \times g$ for 10 min at 4 °C. Total protein concentration was measured by BCA (Thermo Fisher Scientific).

Specific protein expression assays were normalized to total protein amounts for homogenates or equal volumes for culture supernatants and BALs. Amounts of IL-5, IL-9, and IL-13 were quantified by cytometric bead array using a LSRII flow cytometer and FCAP Array analysis software (BD Biosciences). TSLP and IL-33 protein were measured by ELISA (R&D Systems). To quantify TSLP protein in sorted lung populations, the ELISA protocol was modified to avoid spurious measurements due to endogenous biotin in ATII cells.[49] Briefly, cell homogenates were incubated with goat anti-mouse TSLP detection antibodies (R&D Systems) and subsequently probed with horseradish peroxidase (HRP)-conjugated donkey anti-goat IgG antibodies (SouthernBiotech, Birmingham, AL), followed by application of Substrate Solution (R&D Systems). Processing of IL-33 was assessed by western blotting of denatured lung homogenates separated by SDS-polyacrylamide gel electrophoresis with gradient gels (Thermo Fisher Scientific) and transferred to poly(vinylidene fluoride) membranes (EMD Millipore). Membranes were probed with goat anti-mouse IL-33 (R&D Systems) and rabbit anti-mouse β-actin antibodies (Cell Signaling, Danvers, MA), which were detected with HRP-conjugated mouse anti-goat IgG and goat anti-rabbit IgG secondary antibodies (SouthernBiotech). Peroxidase signal was developed using Pierce ECL Substrate (Thermo Fisher Scientific), and data were acquired with a Kodak Image Station 440CF and Kodak Molecular Imaging software. Densitometry analysis was performed using ImageJ software (National Institutes of Health, Bethesda, MD).

RNA isolation and quantitative reverse transcription-PCR. Lung lobes were snap-frozen in liquid nitrogen and homogenized in M tubes in RNAzol (Molecular Research Center, Cincinnati, OH) by gentleMACS, running program "RNA_02". Total RNA was extracted, dissolved in RNase-free water, and purified using RNeasy Mini columns (Qiagen, Venlo, The Netherlands). To isolate RNA from sorted cells, pellets were lysed in RLT Plus, and total RNA was eluted from RNeasy Plus Micro columns (Qiagen). RNA was reverse transcribed with VILO cDNA Synthesis Kit, and the cDNA was used as a template for quantitative reverse transcription-PCR using the Power SYBR Green Kit on a StepOnePlus cycler (Life Technologies). Where indicated, TaqMan probes and the TaqMan Gene Expression Kit were used (Life Technologies). Primers used for SYBR Green PCRs are as follows. *18 s*: 5′-GAAACGGCTACCACATCCAAG-3′, 5′-TTACAGG GCCTCGAAAGAGTC-3′; *Tslp*: 5'-TCGAGGACTGTGAGAGCAA GCCAG-3', 5'-CTGGAGATTGCATGAAGGAATACCA-3'; *Il33*: 5′-GGGCTCACTGCAGGAAAGTA-3′, 5′-GGACCAGGGCTTCGCC T-3′; *Il2*: 5′-TGAGCAGGATGGAGAATTACAGG-3′, 5′-GTCCAAG TTCATCTTCTAGGCAC-3′; *Il7*: 5′-TTCCTCCACTGATCCTTGT TCT-3′, 5′-AGCAGCTTCCTTTGTATCATCAC-3′; *Il9*: 5′-ATGTT GGTGACATACATCCTTGC-3′, 5′-TGACGGTGGATCATCCTT-CAG-3′; *Il5*: 5′-CTCTGTTGACAAGCAATGAGACG-3′, 5′-TCTT CAGTATGTCTAGCCCCTG-3′; *Il13*: 5′-CCTGGCTCTTGCTTG CCTT-3′, 5′-GGTCTTGTGTGATGTTGCTCA-3′; *Muc5ac*: 5′-CA GGACTCTCTGAAATCGTACCA-3′, 5′-AAGGCTCGTACCACA GGGA-3′; *Clca3*: 5′-CTGTCTTCCTCTTGATCCTCCA-3′, 5′-CGTG GTCTATGGCGATGACG-3′; *Tff2*: 5′-TGCTCTGGTAGAGGGCG

AG-3′, 5′-CGACGCTAGAGTCAAAGCAG-3′; *Irf4*: 5′-TCCGACA GTGGTTGATCGAC-3′, 5′-CCTCACGATTGTAGTCCTGCTT-3′.

***Irf4* genotyping**. Presence (Δ*loxP*) or absence (intron 1) of Cre-loxP recombination in the *Irf4* locus was assessed by PCR analysis of tail DNA using the following primers. *Irf4* intron 1: 5′-GAAGGGGC AAGTGTAGAAACAGT-3′, 5′-TTTACATTAACACGCTCCGTTG-3′; *Irf4* Δ*loxP*: 5′-CCATGGTGGCGGGATCCAAT-3′, 5′-CTTCC TCATCTCCGGGCCTTTCG-3′.

Statistical analysis. Statistical analysis was performed as indicated in figure legends using Prism software (GraphPad Software, La Jolla, CA).

SUPPLEMENTARY MATERIAL is linked to the online version of the paper at http://www.nature.com/mi

ACKNOWLEDGMENTS

We thank J-P Girard (University de Toulouse), S Ziegler (Benaroya Research Institute), and M Steinhoff for reagents, M Donne, J Rock and Z-E Wang for technical assistance, N Flores, M Consengco, and M Li for animal care and H Chapman, J Cyster, D Erle, and M Krummel for comments on the manuscript. This work was supported by National Institutes of Health grants AI026918, AI030663, and AI119944, the Howard Hughes Medical Institute, and the Sandler Asthma Basic Research Center at the University of California, San Francisco. A Mohapatra was supported by the UCSF Medical Scientist Training Program.

AUTHOR CONTRIBUTIONS

A.M., S.J.V.D., C.S., and R.M.L. designed experiments. A.M., S.J.V.D., C.S., and J.C.N. conducted the experiments. J.C.N. and H.-E.L. provided reagents. A.M. and R.M.L. wrote the manuscript.

DISCLOSURE

The authors declare no conflict of interest.

REFERENCES

1. Bussink, A.P., Speijer, D., Aerts, J.M. & Boot, R.G. Evolution of mammalian chitinase(-like) members of family 18 glycosyl hydrolases. *Genetics* **177**, 959–970 (2007).
2. Reese, T.A. *et al.* Chitin induces accumulation in tissue of innate immune cells associated with allergy. *Nature* **447**, 92–96 (2007).
3. Van Dyken, S.J. *et al.* Chitin activates parallel immune modules that direct distinct inflammatory responses via innate lymphoid type 2 and gammadelta T cells. *Immunity* **40**, 414–424 (2014).
4. Spits, H. *et al.* Innate lymphoid cells - a proposal for uniform nomenclature. *Nat. Rev. Immunol.* **13**, 145–149 (2013).
5. Chang, Y.J. *et al.* Innate lymphoid cells mediate influenza-induced airway hyper-reactivity independently of adaptive immunity. *Nat. Immunol.* **12**, 631–638 (2011).
6. Monticelli, L.A. *et al.* Innate lymphoid cells promote lung-tissue homeostasis after infection with influenza virus. *Nat. Immunol.* **12**, 1045–1054 (2011).
7. Ikutani, M. *et al.* Identification of innate IL-5-producing cells and their role in lung eosinophil regulation and antitumor immunity. *J. Immunol.* **188**, 703–713 (2012).
8. Nussbaum, J.C. *et al.* Type 2 innate lymphoid cells control eosinophil homeostasis. *Nature* **502**, 245–248 (2013).
9. Fehrenbach, H. Alveolar epithelial type II cell: defender of the alveolus revisited. *Respir Res.* **2**, 33–46 (2001).
10. Wikenheiser, K.A. *et al.* Production of immortalized distal respiratory epithelial cell lines from surfactant protein C/simian virus 40 large tumor antigen transgenic mice. *Proc. Natl Acad. Sci. USA* **90**, 11029–11033 (1993).
11. Price, A.E. *et al.* Systemically dispersed innate IL-13-expressing cells in type 2 immunity. *Proc. Natl Acad. Sci. USA* **107**, 11489–11494 (2010).
12. Wilhelm, C. *et al.* An IL-9 fate reporter demonstrates the induction of an innate IL-9 response in lung inflammation. *Nat. Immunol.* **12**, 1071–1077 (2011).
13. Staudt, V. *et al.* Interferon-regulatory factor 4 is essential for the developmental program of T helper 9 cells. *Immunity* **33**, 192–202 (2010).
14. Klein, U. *et al.* Transcription factor IRF4 controls plasma cell differentiation and class-switch recombination. *Nat. Immunol.* **7**, 773–782 (2006).
15. Gause, W.C., Urban, J.F. Jr. & Stadecker, M.J. The immune response to parasitic helminths: insights from murine models. *Trends Immunol.* **24**, 269–277 (2003).
16. Zhang, Y., Foster, J.M., Nelson, L.S., Ma, D. & Carlow, C.K. The chitin synthase genes chs-1 and chs-2 are essential for C. elegans development and responsible for chitin deposition in the eggshell and pharynx, respectively. *Dev. Biol.* **285**, 330–339 (2005).
17. Licona-Limon, P. *et al.* Th9 cells drive host immunity against gastrointestinal worm infection. *Immunity* **39**, 744–757 (2013).
18. Kuperman, D.A. *et al.* Direct effects of interleukin-13 on epithelial cells cause airway hyperreactivity and mucus overproduction in asthma. *Nat. Med.* **8**, 885–889 (2002).
19. Wills-Karp, M. *et al.* Trefoil factor 2 rapidly induces interleukin 33 to promote type 2 immunity during allergic asthma and hookworm infection. *J. Exp. Med.* **209**, 607–622 (2012).
20. Lee, J.H. *et al.* Interleukin-13 induces dramatically different transcriptional programs in three human airway cell types. *Am. J. Respir. Cell Mol. Biol.* **25**, 474–485 (2001).
21. Eum, S.Y., Maghni, K., Tolloczko, B., Eidelman, D.H. & Martin, J.G. IL-13 may mediate allergen-induced hyperresponsiveness independently of IL-5 or eotaxin by effects on airway smooth muscle. *Am. J. Physiol. Lung Cell Mol. Physiol.* **288**, L576–L584 (2005).
22. Cayrol, C. & Girard, J.P. IL-33: an alarmin cytokine with crucial roles in innate immunity, inflammation and allergy. *Curr. Opin. Immunol.* **31**, 31–37 (2014).
23. Lefrancais, E. *et al.* IL-33 is processed into mature bioactive forms by neutrophil elastase and cathepsin G. *Proc. Natl Acad. Sci. USA* **109**, 1673–1678 (2012).
24. Luzina, I.G. *et al.* Full-length IL-33 promotes inflammation but not Th2 response in vivo in an ST2-independent fashion. *J. Immunol.* **189**, 403–410 (2012).
25. Bessa, J. *et al.* Altered subcellular localization of IL-33 leads to non-resolving lethal inflammation. *J. Autoimmun.* **55**, 33–41 (2014).
26. Rickard, J.A. *et al.* RIPK1 regulates RIPK3-MLKL-driven systemic inflammation and emergency hematopoiesis. *Cell* **157**, 1175–1188 (2014).
27. Ziegler, S.F. *et al.* The biology of thymic stromal lymphopoietin (TSLP). *Adv. Pharmacol.* **66**, 129–155 (2013).
28. Kato, A., Favoreto, S. Jr., Avila, P.C. & Schleimer, R.P. TLR3- and Th2 cytokine-dependent production of thymic stromal lymphopoietin in human airway epithelial cells. *J. Immunol.* **179**, 1080–1087 (2007).
29. Halim, T.Y., Krauss, R.H., Sun, A.C. & Takei, F. Lung natural helper cells are a critical source of Th2 cell-type cytokines in protease allergen-induced airway inflammation. *Immunity* **36**, 451–463 (2012).
30. Mjosberg, J. *et al.* The transcription factor GATA3 is essential for the function of human type 2 innate lymphoid cells. *Immunity* **37**, 649–659 (2012).
31. Moffatt, M.F. *et al.* A large-scale, consortium-based genomewide association study of asthma. *N. Engl. J. Med.* **363**, 1211–1221 (2010).
32. Gauvreau, G.M. *et al.* Effects of an anti-TSLP antibody on allergen-induced asthmatic responses. *N. Engl. J. Med.* **370**, 2102–2110 (2014).
33. Glasmacher, E. *et al.* A genomic regulatory element that directs assembly and function of immune-specific AP-1-IRF complexes. *Science* **338**, 975–980 (2012).
34. Turner, J.E. *et al.* IL-9-mediated survival of type 2 innate lymphoid cells promotes damage control in helminth-induced lung inflammation. *J. Exp. Med.* **210**, 2951–2965 (2013).
35. Steenwinckel, V. *et al.* IL-13 mediates in vivo IL-9 activities on lung epithelial cells but not on hematopoietic cells. *J. Immunol.* **178**, 3244–3251 (2007).
36. Juncadella, I.J. *et al.* Apoptotic cell clearance by bronchial epithelial cells critically influences airway inflammation. *Nature* **493**, 547–551 (2013).
37. Desai, T.J., Brownfield, D.G. & Krasnow, M.A. Alveolar progenitor and stem cells in lung development, renewal and cancer. *Nature* **507**, 190–194 (2014).

38. Rangasamy, T. *et al.* Disruption of Nrf2 enhances susceptibility to severe airway inflammation and asthma in mice. *J. Exp. Med.* **202**, 47–59 (2005).
39. Jang, Y. *et al.* UVB induces HIF-1alpha-dependent TSLP expression via the JNK and ERK pathways. *J. Invest. Dermatol.* **133**, 2601–2608 (2013).
40. Kouzaki, H., Iijima, K., Kobayashi, T., O'Grady, S.M. & Kita, H. The danger signal, extracellular ATP, is a sensor for an airborne allergen and triggers IL-33 release and innate Th2-type responses. *J. Immunol.* **186**, 4375–4387 (2011).
41. Hara, K. *et al.* Airway uric Acid is a sensor of inhaled protease allergens and initiates type 2 immune responses in respiratory mucosa. *J. Immunol.* **192**, 4032–4042 (2014).
42. Demehri, S. *et al.* Notch-deficient skin induces a lethal systemic B-lymphoproliferative disorder by secreting TSLP, a sentinel for epidermal integrity. *PLoS Biol.* **6**, e123 (2008).
43. Pichery, M. *et al.* Endogenous IL-33 is highly expressed in mouse epithelial barrier tissues, lymphoid organs, brain, embryos, and inflamed tissues: in situ analysis using a novel Il-33-LacZ gene trap reporter strain. *J. Immunol.* **188**, 3488–3495 (2012).
44. Carpino, N. *et al.* Absence of an essential role for thymic stromal lymphopoietin receptor in murine B-cell development. *Mol. Cell Biol.* **24**, 2584–2592 (2004).
45. Hoshino, K. *et al.* The absence of interleukin 1 receptor-related T1/ST2 does not affect T helper cell type 2 development and its effector function. *J. Exp. Med.* **190**, 1541–1548 (1999).
46. Mohrs, M., Shinkai, K., Mohrs, K. & Locksley, R.M. Analysis of type 2 immunity in vivo with a bicistronic IL-4 reporter. *Immunity* **15**, 303–311 (2001).
47. Voehringer, D., Shinkai, K. & Locksley, R.M. Type 2 immunity reflects orchestrated recruitment of cells committed to IL-4 production. *Immunity* **20**, 267–277 (2004).
48. Rock, J.R. *et al.* Multiple stromal populations contribute to pulmonary fibrosis without evidence for epithelial to mesenchymal transition. *Proc. Natl Acad. Sci. USA* **108**, E1475–E1483 (2011).
49. Kuhn, C. Biotin stores in rodent lungs: localization to Clara and type II alveolar cells. *Exp. Lung Res.* **14**, 527–536 (1988).